Sains Malaysiana 50(2)(2021): 507-514
http://dx.doi.org/10.17576/jsm-2021-5002-21

Production of Porous Stainless Steel using the Space Holder Method

(Penghasilan Keluli Tahan Karat Berliang menggunakan Kaedah Pengisi Pemegang Ruang)

TAN KOON TATT*, NORHAMIDI MUHAMAD, ANDANASTUTI MUCHTAR, ABU BAKAR SULONG & KOK YIH SHIA

ABSTRACT

Metallic foams and porous materials can be produced by various methods. Among the methods that can produce metallic foams and porous materials, powder metallurgy is a promising method. This study investigates the production of a porous stainless steel by the space holder method in powder metallurgy. A novel space holder i.e. glycine and binder consisting of polymethylmethacrylate and stearic acid are used. Different amounts of glycine are added to the mixture of stainless-steel powder and binder. Subsequently, each mixture is cold-pressed at a pressure of 9-ton m^{-2}. The samples are sintered at 1050 and 1150 °C with holding times of 30, 60, and 90 min. The microstructures and physical and mechanical properties of the sintered samples are investigated. A porous stainless steel with porosity ranging from 30.8 to 51.4% is successfully fabricated. Results show that the glycine content and sintering parameters influence the properties of the porous stainless steel. The sintering temperature significantly affects volumetric shrinkage. Volumetric shrinkage decreases as the volume fraction of glycine increases to 30% whereas sintering temperature 1150 °C and holding time 90 min will increase the volumetric shrinkage. The compressive yield strength and corresponding elastic modulus are in the ranges of 22.9 to 57.6 MPa and 6.3 to 26.8 GPa, respectively. The samples produced have potential biomedical applications because their mechanical properties, yield strength and elastic modulus match those of human bones.

Keywords: Metal foam; porous stainless steel; sintered steel; space holder

ABSTRAK

Logam berbusa dan bahan berliang dapat dihasilkan dengan pelbagai kaedah. Antara kaedah yang boleh menghasilkan logam berbusa dan bahan berliang, metalurgi serbuk adalah kaedah yang berpotensi. Penyelidikan ini mengkaji penghasilan keluli tahan karat berliang dengan kaedah pengisi pemegang ruang melalui metalurgi serbuk. Pengisi pemegang ruang terbaru iaitu glisina dan pengikat yang terdiri daripada polimetil metaklirat dan asid stearik digunakan. Jumlah kuantiti glisina yang berbeza ditambah kepada campuran serbuk keluli tahan karat dan pengikat. Selanjutnya, setiap campuran dimampat-sejuk dengan tekanan 9-ton m^{-2}. Sampel disinter pada 1050 dan 1150 °C dengan masa pensinteran 30, 60 dan 90 minit. Mikrostruktur, sifat fizikal dan sifat mekanikal sampel dikaji. Keluli tahan karat berliang dengan keliangan dari 30.8 hingga 51.4% berjaya dihasilkan. Keputusan menunjukkan bahawa kandungan glisina dan parameter pensinteran mempengaruhi sifat keluli tahan karat berliang. Suhu pensinteran sangat menpengaruhi pengecutan isi padu. Pengecutan isi padu menurun apabila pecahan isi padu glisina meningkat kepada 30% sedangkan suhu pensinteran 1050 °C dan masa pensinteran 90 minit akan meningkatkan pengecutan isi padu. Kekuatan mampatan dan modus anjal adalah dalam lingkungan 22.9 ke 57.6 MPa dan 6.3 ke 26.8 GPa. Sampel yang dihasilkan berpotensi diaplikasikan dalam bidang bioperubatan kerana sifat mekanikalnya: Kekuatan mampatan dan modulus anjal sepadan dengan sifat mekanikal tulang manusia.

Kata kunci: Keluli disinter; keluli tahan karat berliang; logam berbusa; pengisi pemegang ruang

INTRODUCTION

In recent years, the production of metallic implants has attracted considerable attention. Metals and alloys are suitable for biomedical applications because of their good mechanical properties and effective corrosion resistance. However, the elastics modulus of metal is considerably greater than that of natural bone (10 to 30 GPa) (Bhattarai et al. 2008; Dewidar et al. 2007; Heary et al. 2017). This mismatch causes stress shielding, which leads to bone resorption and implant loosening (Bhattarai et al. 2008; Cetinel et al. 2019; Wahab et al. 2018). At present, porous metals are fabricated for biomedical applications to overcome this problem. The use of porous metals as metallic implants reduces the stress shielding effect, resulting in the prolongation of the implant lifetime. Moreover, the open-cellular structure of porous metals permits the ingrowth of new bone tissue and the transport of body fluids. The advantage of porous metals is their capability to provide biological anchorage for the surrounding body tissue via the ingrowth of mineralized tissue into the pore space (Dewidar et al. 2007).

At present, 316L stainless steel is widely used in metallic implants because of its good mechanical properties and reasonable cost. Specifically, 316L stainless steel is used in acetabula cup (one half of an artificial hip joint) applications (Dewidar et al. 2007; Manam et al. 2017). Porous stainless steels are generally manufactured through powder metallurgy (PM) methods, such as loose powder sintering, hollow powder sintering, selective laser sintering, and space holder method. Several authors (Abudullah et al. 2017; Bakan 2006; Bekoz & Oktay 2012; Joshi 2019; Mutlu & Oktay 2011; Wahab et al. 2018) have successfully produced a porous stainless steel with the porosity ranging from 39 to 72% *via* the space holder method. In this method, the space holder serves as a pore former, which is removed at low temperature prior to sintering. The pore size and pore shape of a porous stainless steel can be easily adjusted by controlling the shape and size of the space holder.

One of the major issues concerning the space holder method is the selection of an appropriate space holder. The common materials used as a space holder are carbamide [$(NH_2)_2CO$], ammonium bicarbonate [$(NH_4)HCO_3$], and sodium chloride (NaCl). Different types, sizes, and shapes of space holders yield porous metals with different physical and mechanical properties. Bekoz and Oktay (2012) studied the effects of space holder shape on stainless steel foams and obtained stainless steel foam with spherical pores that shows high compressive strength. However, low-cost space holders, such as NaCl powder and ammonium bicarbonate, are difficult to remove completely; the residue can lead to corrosion of the base metal (Bakan 2006; Tan 2016). The decomposition of a space holder at high temperatures is not favorable because the crack products might contaminate the base metal. An ideal space holder must be compatible with the processing conditions.

In recent years, the space holder method has been improved by controlling the process parameters. Nonetheless, the process can be further improved by exploring a new type of space holder, which is the objective of the present study. Specifically, this study aims to produce porous stainless steels for biomedical applications. The effect of space holder content and sintering parameters on the physical and mechanical properties of porous stainless steels is discussed.

Materials and Methods

Water-atomized 316L stainless steel powder with a particle size of D_{50} = 17 µm (supplied by EPSON ATMIX, Japan), and glycine (supplied by Fisher Scientific) with a particle size ranging from 75 to 150 µm were used. Glycine is appropriate because it is a low-cost, non-toxic amino acid that can be produced with high purity (Abdel Ghanyl et al. 2011; Tatt et al. 2012). Furthermore, it can be removed easily by dissolution or thermal decomposition because of its high solubility in water and low decomposition temperature. A binder (9% wt.) consisting of polymethylmethacrylate and stearic acid was added to increase the strength of the green compact. The binder and powders were mixed by a sigma-type blade mixer for 1 h 45 min. To study the effect of space holder content, three feedstocks with different volume fractions of glycine (10, 20, and 30%) were prepared.

Subsequently, the feedstocks were uniaxially cold-pressed at a pressure of 9-ton m^{-2} into green compacts with the size of 15 mm ø × 20 mm L. All binders and space holders were removed by solvent debinding. This procedure was performed by immersing the compacts in distilled water at 70 °C for 56 h. Finally, the green compacts were sintered in pure argon at 1050 and 1150 °C with holding times of 30, 60, and 90 min. Six sample groups (Table 1) were prepared.

The microstructures of the sintered samples were characterized by scanning electron microscopy (SEM), and the densities and porosities of the samples were measured using the Archimedes water immersion method, ISO 2738. Compression tests (JIS H7902) were carried out using a 100-ton universal tensile testing machine with a strain rate of 0.75 mm min^{-1}. For the hardness HRL (MPIF standard 43) properties, a macroscopic hardness tester was used to test three samples from each group. The load was 588.4 N, and the indentor was a 1/8 in ball.

Results and Discussion

Physical Properties and Microstructure Analysis

As shown in Table 2, a porous stainless steel with porosity that ranges from 30.8 to 51.4% is fabricated. The sintering holding time elicits no significant effect on porosity. This result can be explained by the comparable porosity of S1 and S3. Both samples were sintered at the same temperature, but with different holding times and space holder contents. Theoretically, longer sintering time reduces porosity (Chu et al. 2017; Dewidar 2012; German 1996; Ramli et al. 2018). Although S3 was sintered for a longer time than S1, the former still displays higher porosity than the latter. This result is due to the higher space holder content used in S3 than in S1. A similar result was observed when S4 and S6 were compared. These results indicate that holding time does not significantly affect the physical properties of the porous stainless steel.

S1, S3, and S5 were sintered at 1050 °C. The difference in average porosity among these samples is approximately 5%. In general, porosity increases with the increase in glycine content. Table 2 shows that the difference in average porosity between S4 and S6 is 8.7%. This finding shows that the effect of space holder content on porosity is more pronounced when the samples are sintered at 1150 °C than at other temperatures. At 1150 °C, more sintering activity occurs, thereby improving densification and reducing porosity.

The volumetric shrinkage of the samples is mainly due to spaces created by the presence of glycine and consolidation of powder due to sintering. The effect of glycine content on the volumetric shrinkage is not significant because the shrinkage difference is small. At 1050 °C, the volumetric shrinkage fluctuates, the variation of which is less than 1.5%. However, the volumetric shrinkage linearly decreases as the volume fraction of glycine increases at 1150 °C. The observation is inconsistent with the finding obtained by Manonukul et al. (2010) and Su et al. (2017). This is because the growth of large pores retards the sintering activity and reduces the volumetric shrinkage. Furthermore, Manonukul et al. (2010) also found that the volume fraction of metal powder used must be more than 25% to retain the foam structure. Although glycine content is greater in S6 than in the other samples, the metal powder retained the porous structure. Sintering temperature and holding time also significantly affect the volumetric shrinkage. Increasing the sintering temperature will increase the volumetric shrinkage. Su et al. (2017) obtained the similar finding. Table 2 indicates that the samples sintered at high temperatures and long holding times (S2 and S6) have great volumetric shrinkage. The results show that increasing sintering temperature by 100 °C would increase volumetric shrinkage by nearly 10%.

The SEM images of the porous stainless are shown in Figure 1. S5 shows only slight necking of particles because the sample is sintered at a low temperature of 1050 °C. In addition, S5 has a large pore size because of the short sintering time and large volume of the space holder used. Low sintering temperature and short sintering time provide low activation energy for sintering. Two types of pores can be observed in the samples. One type is the small micropore, which results from incomplete sintering of metal powder. Micropores are isolated and found in all samples. Another type is the interpenetrating macropore (>100 μm). The morphology of the macropore corresponds with the glycine particle. This result suggests that the macropore structure can be easily tailored by the proper selection of size, shape and content of glycine particles.

As shown in Figure 1(b), 1(d) and 1(f), the number of macropores decreases when the samples are sintered at 1150 °C. Conversely, extremely large pores are found in S4 and S6. As previously discussed, this phenomenon can be attributed to pore coalescence. A comparison between Figure 1(a) and 1(c) shows that the grain of the latter is larger than the former. This result can be attributed to the longer sintering time of S3 than S1. *In vivo*, an interconnection size of more than 50 μm can aid the bone formation and penetration of body fluid (Chen et al. 2009; Zhang et al. 2018). The interpenetrating macropore formed in the samples has a size greater than 100 μm. Thus, the porous stainless steel produced in this study is suitable for biomedical applications.

MECHANICAL PROPERTIES

The compressive behavior of all samples is shown in Figure 2. The compressive stress-strain curve for a typical porous metal is characterized by three regions: Elastic region where stress increases linearly, a long plateau region with nearly constant flow stress, and a densification region with rapidly increasing flow stress (Cetinel et al. 2019; Mutlu & Oktay 2011; Osman et al. 2017; Tatt et al. 2016; Wang et al. 2018). In the elastic region, bending of cell walls occurs. After the yield point, the collapsed cell edge bends easily at low stress, forming large strains.

This behavior is extremely important for some functional applications like energy absorbers and bear-loading material in biomedical applications. At the end of the plateau region, the stress rapidly increases because the pores are flattened and cell walls come into contact with one another (Mutlu & Oktay 2011; Wang et al. 2018). Figure 2 shows that the low-porosity sample curves and the high-porosity sample curves significantly differ. S5 displays an obvious plateau region compared with the other curves. Although other sample curves possess considerably high porosity, the plateau regions are less noticeable. This result implies that the number of broken walls of these samples is less and the pores are distributed unevenly. Consequently, the stress concentration region is mini-mized, and the samples' bulk-like properties are enhanced.

By theory, the mechanical properties of cellular materials are related to their relative density ρ/ρ_{ys}, where ρ is the density of the cellular materials and ρ_{ys} is the density of the bulk material. The Gibson-Ashby model (Ashby et al. 2000; Mutlu & Oktay 2011; Yi et al. 2018) can be used to describe the mechanical behavior of porous metals (Table 3). If the compressive yield strength σ_{ys} and elastic modulus E_{ys} of a bulk metal are known, the corresponding properties σ_{pl} and E_{pl} of the porous metal can be predicted. Gibson and Ashby proposed that the relative density exponents of 1.5 and 2 should be used in their models. For the constant values, 0.3 for the compressive yield strength and 1 for the elastic modulus are commonly used by researchers (Dewidar et al. 2007; Wen et al. 2002; Yi et al. 2018).

Previous studies (Bekoz & Oktay 2012; Dewidar et al. 2007; Tan 2016) found that the empirical data do not fit with those derived through the theoretical model because the Gibson-Ashby model assumes pore walls to be a solid material and because the porous metals have different deformation behaviors. To best describe the mechanical properties of porous stainless steel in the present study, the experimental data were analyzed statistically. The models obtained are shown in Table 3. Both models show high R^2 values, indicating that the models are suitable to describe the mechanical behavior. Furthermore, the constants of the models agree with those of the theoretical models. The uses of these models are subject to pore morphology and imperfection in porous structure. Imperfections, such as broken walls and anisotropic pore structure, significantly affect the mechanical properties (Mutlu & Oktay 2011; Seuba et al. 2016).

The compressive yield strength and elastic modulus of all samples are presented in Table 4. S2 and S4 show higher strength and elastic modulus than the other samples. Both samples sintered at a high temperature of 1150 °C show improved densification and mechanical properties. According to Abudullah et al. (2017) and Ramli et al. (2018), sintering at a high temperature will improve densification. These results also agree with the microstructure characteristics of the samples. In general, the mechanical properties increase with the increase in sintering temperature and the decrease in glycine content.

In designing the biomedical implant, the elastic modulus of material must be given special attention. High stiffness implants will cause the surrounding living tissue to sustain excessive load. This phenomenon will eventually lead to implant loosening and implant failure. Although S3 and S5 have poor strength and low elastic modulus, their properties are comparable with those of natural bone. The elastic modulus of both samples, especially S5, is very close to that of human cancellous bone. The effective matching of elastic modulus would prevent stress shielding. In addition, the strength of both samples ranges from 22.9 to 32.1 MPa, which is presumably sufficient to support implantation and *in vivo* loading. The hardness of the samples is affected by porosity. The measured hardness values range from 13.1 to 80.7 HRL. Figure 3 shows that hardness decreases as porosity increases. S2, with the lowest porosity, shows the highest hardness value, whereas S5, with the highest porosity, shows the lowest hardness value. The volume fraction of metal powder decreases with the increase in porosity. This phenomenon yields high-porosity samples with low resistance to shape change when force is applied. The hardness of one sample deviates from the porosity-hardness function. Although the porosity of this sample is low, it shows a higher hardness value. This result can be attributed to the different pore geometries and uneven pore distribution. Most pores in this sample might be concentrated at the inner part. As a result, the surface can sustain greater load.

TABLE 1. Sintering condition

Sample	Sample abbreviation	Volume fraction of space holder (%)	Sintering time (°C)	Holding time (min)
1	S1	10	1050	60
2	S2	10	1150	90
3	S3	20	1050	90
4	S4	20	1150	30
5	S5	30	1050	30
6	S6	30	1150	60

TABLE 2. Effect of processing parameters on porosity and volumetric shrinkage

Sample	Volume fraction of space holder (%)	Porosity (%)	Volumetric shrinkage (%)
S1	10	41.2±1.5	10.3±2.4
S2	10	30.8±5.3	24.3±5.3
S3	20	45.3±1.5	11.5±2.5
S4	20	37.9±2.0	22.0±2.6
S5	30	51.4±1.3	10.9±2.2
S6	30	46.6±5.6	18.5±8.8

TABLE 3. Experimental models for mechanical behaviors

Gibson-Ashby model	Experimental model	R^2
$\frac{\sigma_{pl}}{\sigma_{ys}} = (0.1\text{-}1.0)(\frac{\rho}{\rho_{ys}})^{1.5}$	$\frac{\sigma_{pl}}{\sigma_{ys}} = (0.604)(\frac{\rho}{\rho_{ys}})^{1.5}$	0.97
$\frac{E_{pl}}{E_{ys}} = (0.1\text{-}4.0)(\frac{\rho}{\rho_{ys}})^{2}$	$\frac{E_{pl}}{E_{ys}} = (0.281)(\frac{\rho}{\rho_{ys}})^{2}$	0.96

TABLE 4. Experimental models for mechanical behaviors

Materials	Compressive yield strength (MPa)	Elastic modulus (GPa)
S1	55.5±9.2	19.2±10.5
S2	57.6±42.6	26.8±12.2
S3	32.1±7.0	11.6±1.3
S4	56.9±29.7	25.8±18.0
S5	22.9±2.6	6.3±2.5
S6	46.8±6.0	16.7±8.3
Cancellous bone: Femoral head [14]	32	4.9
Cancellous bone: Vertebra [14]	4.1	1.5

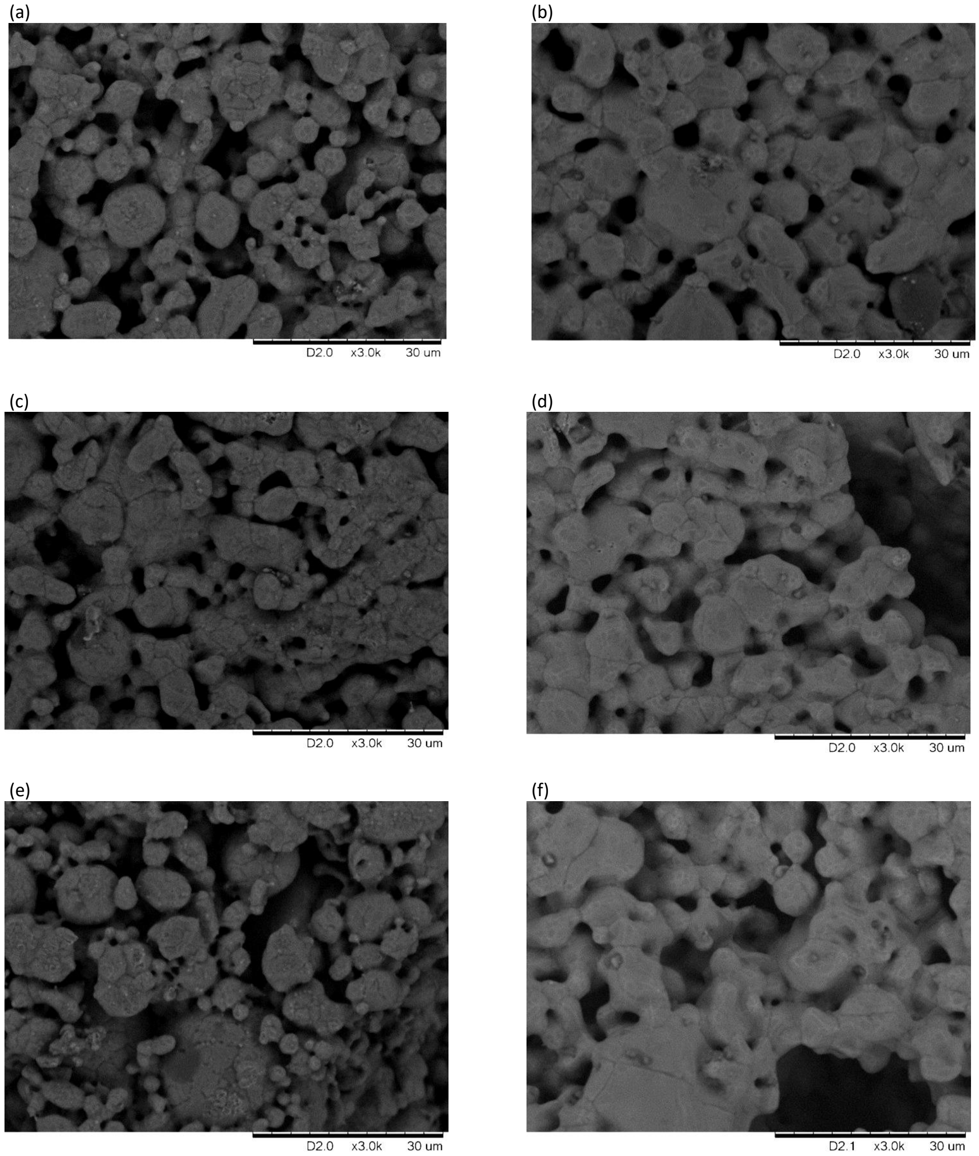

FIGURE 1. SEM images of porous stainless steel showing different pore morphologies: (a) S1; (b) S2; (c) S3; (d) S4; (e) S5; (f) S6

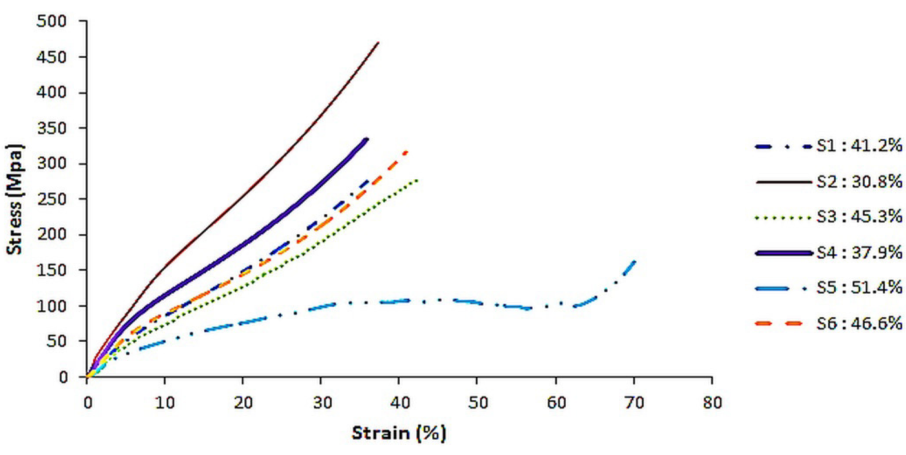

FIGURE 2. Compressive stress-strain curves for porous stainless steel with different porosities

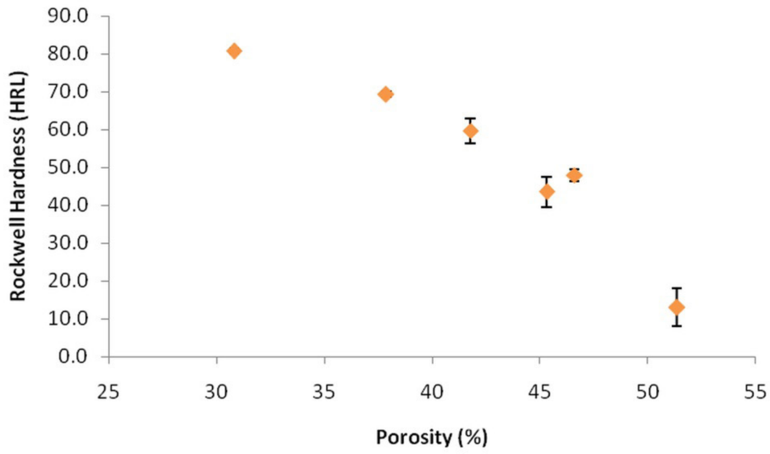

FIGURE 3. Hardness versus porosity of sintered porous stainless steel

CONCLUSION

In this study, porous stainless steels with porosity in the range of 30.8 to 51.4% were successfully manufactured *via* the space holder method. The experimental results highlight the following: Glycine powder is a suitable as a novel space holder that can be used to produce porous stainless steel with different porosities. The physical and mechanical properties of porous stain-less steel can be adjusted by controlling the glycine content. S3 and S5 are suitable for biomedical applications. Process parameters, such as space holder content and sintering temperature, affect the properties of porous stainless steel. The mechanical properties of the samples decrease with the increase in glycine content, but improve with the increase in sintering temperature. Sintering temperature significantly affects the volumetric shrinkage of the samples.

ACKNOWLEDGEMENTS

This work was supported by Universiti Kebangsaan Malaysia Research Grants (UKM-AP-NBT-11-2009 and DIP-2012-029).

REFERENCES

Abdel Ghanyl, N.A., El-Shenawy, A.E. & Hussien, W.A.M. 2011. The inhibitive effect of some amino acids on the corrosion behaviour of 316L stainless steel in sulfuric acid solution. *Modern Applied Science* 5(4): 19-29.

Abdullah, Z., Ahmad, S. & Ramli, M. 2017. The impact of composition and sintering temperature for stainless steel foams (ss316l) fabricated by space holder method with urea as space holder. *Materials Science Forum* 888: 413-417.

Ashby, M.F., Evans, A.G., Fleck, N.A., Gibson, L.J., Hutchison, J.W. & Wadley, H.N.G. 2000. *Metal Foams-A Design Guide*. Butterworth-Heinemann: Elsevier. pp. 1-247.

Bakan, H.I. 2006. A novel water leaching and sintering process for manufacturing highly porous stainless steel. *Scripta Materialia* 55(2): 203-206.

Bekoz, N. & Oktay, E. 2012. Effects of carbamide shape and content on processing and properties of steel foams. *Journal of Materials Processing Technology* 212(10): 2109-2116.

Bhattarai, S.R., Khalil, K.A., Dewidar, M., Hwang, P.H., Yi, H.K. & Kim, H.Y. 2008. Novel production method and *in-vitro* cell compatibility of porous Ti-6Al-4V alloy disk for hard tissue engineering. *Journal of Biomedical Materials Research Part A* 86(2): 289-299.

Cetinel, O., Esen, Z. & Yildirim, B. 2019. Fabrication, morphology analysis, and mechanical properties of Ti foams manufactured using the space holder method for bone substitute materials. *Metals* 9(340): 1-12.

Chen, L., Li, T., Li, Yi-Min, He, H. & Hu, You-Hua. 2009. Porous titanium implants fabricated by metal injection molding. *Transactions of Nonferrous Metals Society of China* 19(5): 1174-1179.

Chu, Z., Jia, C., Liu, J., Ding, R. & Yuan, G. 2017. Effects of sintering time on microstructure and properties of alumina foam ceramics. *Journal of Ceramic Science and Technology* 8(4): 499-504.

Dewidar, M. 2012. Influence of processing parameters and sintering atmosphere on the mechanical properties and microstructure of porous 316L stainless steel for possible hard-tissue applications. *Journal of Mechanical & Mechatronics Engineering IJMME-IJENS* 12(1): 10-24.

Dewidar, M.M., Khalil, A.K. & Lim, J.K. 2007. Processing and mechanical properties of porous 316L stainless steel for biomedical applications. *Transactions of Nonferrous Metals Society of China* 17(3): 468-473.

German, R.M. 1996. *Sintering Theory and Practice*. 5th ed. New York, USA: Wiley-Interscience Publication. pp. 1-232.
Gibson, L.J. & Ashby, M.F. 1997. Thermal, electrical and acoustic properties of foams. In *Cellular Solids: Structure and Properties.* 2nd ed. New York: Cambridge University Press. pp. 283-308.
Heary, R.F., Parvathreddy, N., Sampath, S. & Agarwal, N. 2017. Elastic modulus in the selection of interbody implants. *Journal of Spine Surgery* 3(2): 163-167.
Joshi, S. 2019. Comparative analysis of characteristics of stainless-steel cellular material prepared through powder metallurgy using accicular and crushed urea as space holder. *Material Science Research India* 16(2): 183-188.
Manam, N.S., Harun, W.S.W., Shri, D.N.A., Ghani, S.A.C., Kurniawan, T., Ismail M.H. & Ibrahim, M.H.I. 2017. Study of corrosion in biocompatible metals for implants: A review. *Journal of Alloys and Compounds* 701: 698-715.
Manonukul, A., Muenya, N., Léaux, F. & Amaranan, S. 2010. Effects of replacing metal powder with powder space holder on metal foam produced by metal injection moulding. *Journal of Materials Processing Technology* 210(3): 529-535.
Mutlu, I. & Oktay, E. 2011. Production and characterisation of Cr-Si-Ni-Mo steel foams. *Indian Journal of Engineering & Materials Sciences* 18: 227-232.
Osman, H.A., Omran, A.M., Atlam, A.A., Sulong, A.B. & Kh, M.M. 2017. Characterization of aluminium foam produced from aluminium scrap by using $CaCo_3$ as foaming agent. *Journal of Engineering Sciences* 45(4): 448-459.
Ramli, M.I., Sulong, A.B., Muhamad, N., Muchtar, A., Arifin, A., Mohd Foudzi, F. & Hammadi Al-Furjan, M.S. 2018. Effect of sintering parameters on physical and mechanical properties of powder injection moulded stainless steel-hydroxyapatite composite. *PLoS ONE* 13(10): e0206247.
Seuba, J., Deville, S., Guizard, C. & Stevenson, A.J. 2016. Mechanical properties and failure behavior of unidirectional porous ceramics. *Scientific Reports* 6(24326): 1-11.
Su, M.Z., Wang, H.M. & Chen, C. 2017. Effects of micropores on processing and properties of porous irons. *Applied Mechanics and Materials* 863: 26-32.
Tan, K.T. 2016. Penghasilan keluli tahan karat SS316L berbusa melalui kaedah pengisi pemegang ruang-pengacuanan suntikan logam. PhD Thesis, Fakulti Kejuruteraan dan Alam Bina, Universiti Kebangsaan Malaysia (Unpublished).
Tatt, T.K., Muhamad, N., Muchtar, A., Sulong, A.B. & Cherng, N.M. 2016. Influence of sintering parameters on the compressive yield strength of stainless-steel foams produced by the space holder method. *Sains Malaysiana* 45(4): 653-658.
Tatt, T.K., Muhamad, N., Muchtar, A., Sulong, A.B. & Yunn, H.S. 2012. Rheological behavior of novel feedstock for manufacturing porous stainless steel via (MIM)-PSH. *Jurnal Teknologi (Sciences and Engineering)* 59: 187-191.
Wahab, N.A., Ahmad, I.N., Omar, N.F., Zainal, N.F.A. & Loganathan, T.M. 2018. Processing of porous 316L stainless steel by replacing metal powder with saccharose. *International Journal of Engineering & Technology* 7(4.18): 232-236.
Wang, J., Wang, N., Liu, X., Ding, J., Xia, X., Chen, X. & Zhao, W. 2018. Compressive deformation behavior of closed-cell micro-pore magnesium composite foam. *Materials* 11(731): 1-14.
Wen, C.E., Mabuchi, M., Yamada, Y., Shimojima, K., Chino, Y., Asahina, T. & Mabuchi, M. 2002. Processing and mechanical properties of autogenous titanium implant materials. *Journal of Materials Science: Material in Medicine* 13: 397-401.
Yi, Y., Zheng, X., Fu, Z., Wang, C., Xu, X. & Tan, X. 2018. Multi-scale modeling for predicting the stiffness and strength of hollow-structured metal foams with structural hierarchy. *Materials* 11(380): 1-12.
Zhang, K., Fan, Y., Dunne, N. & Li, X. 2018. Effect of microporosity on scaffolds for bone tissue engineering. *Regenerative Biomaterials* 5(2): 115-124.

Tan Koon Tatt*
Faculty of Engineering & Built Environment
MAHSA University, Bandar Saujana Putra
42610 Jenjarom, Selangor Darul Ehsan
Malaysia

Tan Koon Tatt*
School of Science & Technology
Wawasan Open University
54, Jalan Sultan Ahmad Shah
10050 Penang
Malaysia

Norhamidi Muhamad, Andanastuti Muchtar, Abu Bakar Sulong & Kok Yih Shia
Centre for Materials Engineering and Smart Manufacturing
Department of Mechanical and Materials Engineering
Faculty of Engineering and Built Environment
Universiti Kebangsaan Malaysia
43600 UKM Bangi, Selangor Darul Ehsan
Malaysia

*Corresponding author; email: sean@mahsa.edu.my

Received: 10 January 2020
Accepted: 27 July 2020